J. Basic. Appl. Sci. Res., 2(8)7516-7525, 2012

ISSN 2090-4304
Journal of Basic and Applied Scientific Research
www.textroad.com

Microstructure, Phase Transition Temperature and Electrical Properties of Pure and Tin Modified $(Bi_{0.5}Na_{0.5})_{0.94}Ba_{0.06}TiO_3$ Lead Free Ferroelectric Ceramics

Enyew Amare Zereffa*, A.V. Prasadarao

Department of Inorganic and Analytical Chemistry, College of Science and Technology, Andhra University, Visakhapatnam – 530003

ABSTRACT

Ceramic samples with general formula $(Bi_{0.5}Na_{0.5})_{0.94}Ba_{0.06}Ti_{1-x}Sn_x)O_3$ (for x = 0.0,0.005,0.015 and 0.03) were synthesized by the conventional ceramic method. Microstructure, dielectric properties, impedance and conductivity studies were performed. The entire samples formed pure phase with rhombohedral structure. Grain size varied with the increase of Sn content. The Curie temperature, T_c, got shifted to higher temperature as the amount of dopant increased. Dielectric studies revealed that doping with low concentration of tin (0.5mol %) enhanced dielectric properties. A.C impedance studies indicated the bulk resistance was shown to decrease with increasing temperature and tin concentration resulting in a negative temperature coefficient of resistance (NTCR) behavior for the above materials.

Keywords: Grain size; Dielectric constant; Ferroelectric properties; Sintering

1. INTRODUCTION

Ferroelectric bismuth sodium titanate, $Bi_{0.5}Na_{0.5}TiO_3$ (BNT), was first reported by Smolenski [1] to have a rhombohedral structure with a large remnant polarization (Pr=38μC/cm^2) at room temperature and a high Curie temperature T_C =320°C [2-3].

Subsequently, due to the increasing demand to develop lead free piezoelectric ceramics to replace lead based ceramics for fabrication of ferroelectric and piezoelectric devices, BNT has evolved as a potential candidate. Besides this, BNT also undergoes two phase transitions one from ferroelectric to antiferrolectric near 200^{o}C and the other from antiferroelectric to paraelectric phase around 320^{o}C. However, the large coercive field (E_c=73 kV/cm) and relative high conductivity associated with BNT limit its use for potential electromechanical devices.

These problems were reduced either by forming solid solution of BNT with $BaTiO_3$[4], $NaNbO_3$[5], $BiFeO_3$[6], $KNbO_3$ [7] or by adding some modifier of transition metal oxides such as ZrO_2 [8] ,Nb_2O_5 [9],MnO_2 [10] and rare earth oxides like La_2O_3[11],Eu_2O_3[12] to decrease the conductivity or coercive field. Among the various solid solutions of BNT, bismuth sodium barium titanate $(Bi_{0.5}Na_{0.5})_{1-x}Ba_xTiO_3$ (BNBT) was found to form a rhombohderal- tetragonal morphotropic phase boundary (MPB) near x = 0.06 that showed enhanced piezoelectric properties [2]. This composition has a higher coercive field and medium piezoelectric constant when compared to PZT.

In the case of a similar perovskite type compound $BaTiO_3$, it was well established that the substitution of Sn in the form of $Ba(Ti_{1-x}Sn_x)O_3$ lowers the Curie temperature from 120^{o}C to room temperature and causes a pinching of other phase transformations in it. Though several transition metals oxide and rare earth oxides have been studied to modify the properties of BNT, no study has been reported on tin substitution in BNT or BNBT.

In this paper we report the effect of Sn substitution on the texture, dielectric, impedance, transition temperature and conductivity properties of BNBT.

The remainder of the paper was organized as follows: section II is about experimental details, section III is devoted to results & discussion and the important conclusions are presented in section IV.

2. Experimental

Samples of $(Bi_{0.5}Na_{0.5})_{0.94}Ba_{0.06}Ti_{1-x}Sn_x)$ O_3 with x = 0.0, 0.005,0.015 and 0.03 (abbreviated as BNBTSx) were prepared by the conventional solid state method. The starting raw materials were A.R grade Na_2CO_3, TiO_2, Bi_2O_3, $BaCO_3$, and SnO_2. As per stoichiometric ratios the powders were weighed and mixed well in methanol medium in an agate mortar and calcined at 850 °C for 3 hrs. An extra amount of 3 wt% Bi_2O_3 and Na_2CO_3 were added to the initial mixture to compensate for the respective losses of bismuth and sodium at high sintering temperature. The

***Corresponding Author:** Enyew Amare Zereffa, A.V. Prasadarao, Department of Inorganic and Analytical Chemistry, College of Science and Technology, Andhra University, Visakhapatnam – 530003 E mail: enyewama@yahoo.com

calcined powders were reground and mixed with polyvinyl alcohol (3%) as binder and then pelletized. After burning the binder at 500°C for 1hr, the green bodies were sintered in a closed platinum crucible at 1150°C for 2 hrs with heating and cooling rate of 5°C per minute. Silver paste was annealed on the surfaces of the pellets as electrodes at 600°C for 1hr. Phase identification of the samples was investigated by X-ray powder diffraction (PANalytical-X'Pert PRO, Japan). Microstructure of the ceramic samples was studied by a scanning electron microscope (JEOL-JSM-6610LV, Tokyo, Japan). Measurement of capacitance(C), loss tangent (tanδ) ,complex impedance (Z*), phase angle, Quality factors and resistance (R) in parallel and series were obtained up to 400°C temperature in the frequency range of 100 Hz - 1 MHz obtained using phase sensitive multi meter (N4L PSM 1700) Japan with heating rate of 5°C/min. Samples with composition x = 0, 0.005, 0.015 and 0.03 in $(Bi_{0.5}Na_{0.5})_{0.94}Ba_{0.06}(Ti_{1-x}Sn_x)O_3$ will be denoted in subsequent discussion as BNBT, BNBTS05, BNBTS1.5 and BNBTS3 respectively.

3. RESULTS AND DISCUSSIONS

3.1 X-Ray Diffraction Analysis

Figure 1 depicts x-ray diffraction patterns for $(Bi_{0.5}Na_{0.5})_{0.94}Ba_{0.06}Ti_{1-x}Sn_x)O_3$ powder samples calcined at 850 °C. XRD data is in good agreement with that of rhombohderal precursor (JCPDS file number36-0340) indicated the formation of phase pure samples without any contamination. The apparent particle size and lattice strain of BNBTSx for x 0.0, 0.005, 0.015 and 0.03 were estimated from the X-ray diffraction peak broadening by using the Williamson–Hall approach [13]. The apparent particle size and lattice strain were found to be 44.2 nm, 46.6 nm, 52.3nm, 59.4 nm and 0.0016 .0.0028, 0.0031, 0.0038 corresponding to the concentration of tin or with the value of x = 0.0, 0.005, 0.015 and 0.03 respectively.

3.2 Scanning Electronic Micrographs

The scanning electronic micrographs (SEM) of fractured surfaces of sintered pellets of BNBT doped with different amounts of Sn (x = 0.0, 0.005, 0.015, and 0.03 mol) are shown in Fig 2. From the SEM micrographs it may be noted that the grain size increases initially with addition of small amount of tin but with addition of tin in large concentration to the system, the grain size started decreasing. The average grain size was found to be in the range of 1.2µm, 2.8µm, 2.6µm and 1.4µm respectively.

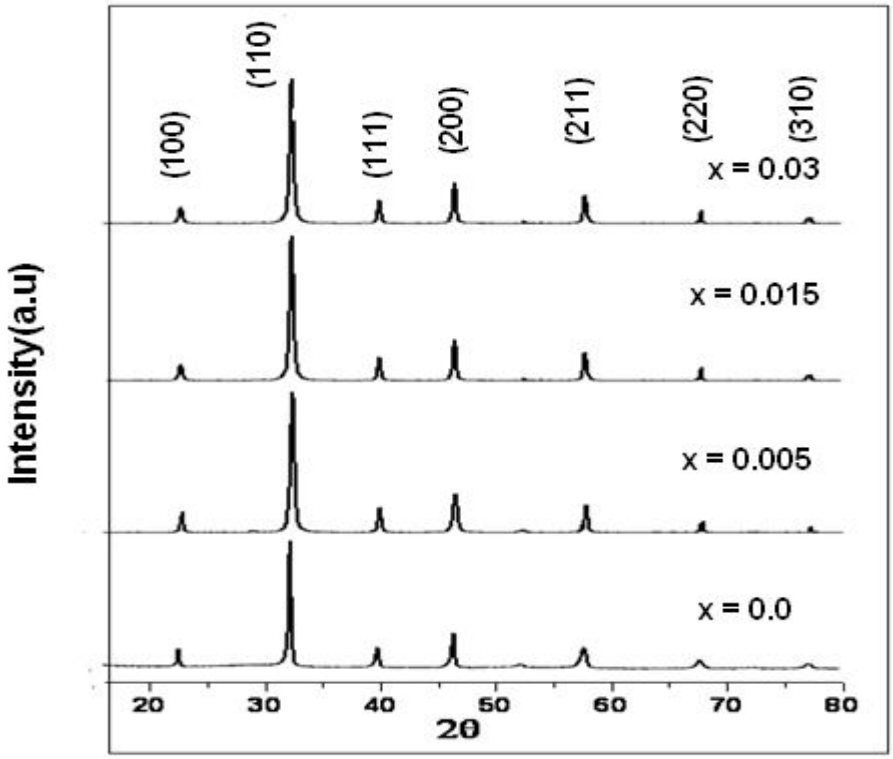

Fig.1 X-Ray Diffraction patterns of $(Bi_{0.5}Na_{0.5})_{0.94}Ba_{0.06}Ti_{1-x}Sn_x)O_3$ ceramic samples calcined at 850 °C for x = 0.0, 0.005, 0.015 and 0.03.

3.3 Dielectric properties

Figure 3 depicts the relative permittivity (ε') and dielectric loss tangent (tanδ) measured at 1, 10 and 50 KHz as a function of temperature for sintered BNBTSx samples where x = 0.0, 0.005 and 0.03. From this figure, it may be seen that with increase of frequency the magnitude of dielectric constant decreased and this is more significant at peak temperatures. The relative permittivity values of the BNBTSx samples were also affected by concentration of tin. For instance, BNBT doped with Sn corresponding to $(Bi_{0.5}Na_{0.5})_{0.94}Ba_{0.06}(Ti_{1-x}Sn_x)O_3$ where x = 0.005 exhibited ε'max value of approximately 11,626 while tin doped with x = 0.03 showed the lowest value (or ε'max ~ 4,696) in the studied temperature range at the same frequency. The reason for high relative dielectric constant obtained for BNBTS05 sample is probably due to the formation of larger grains during sintering.

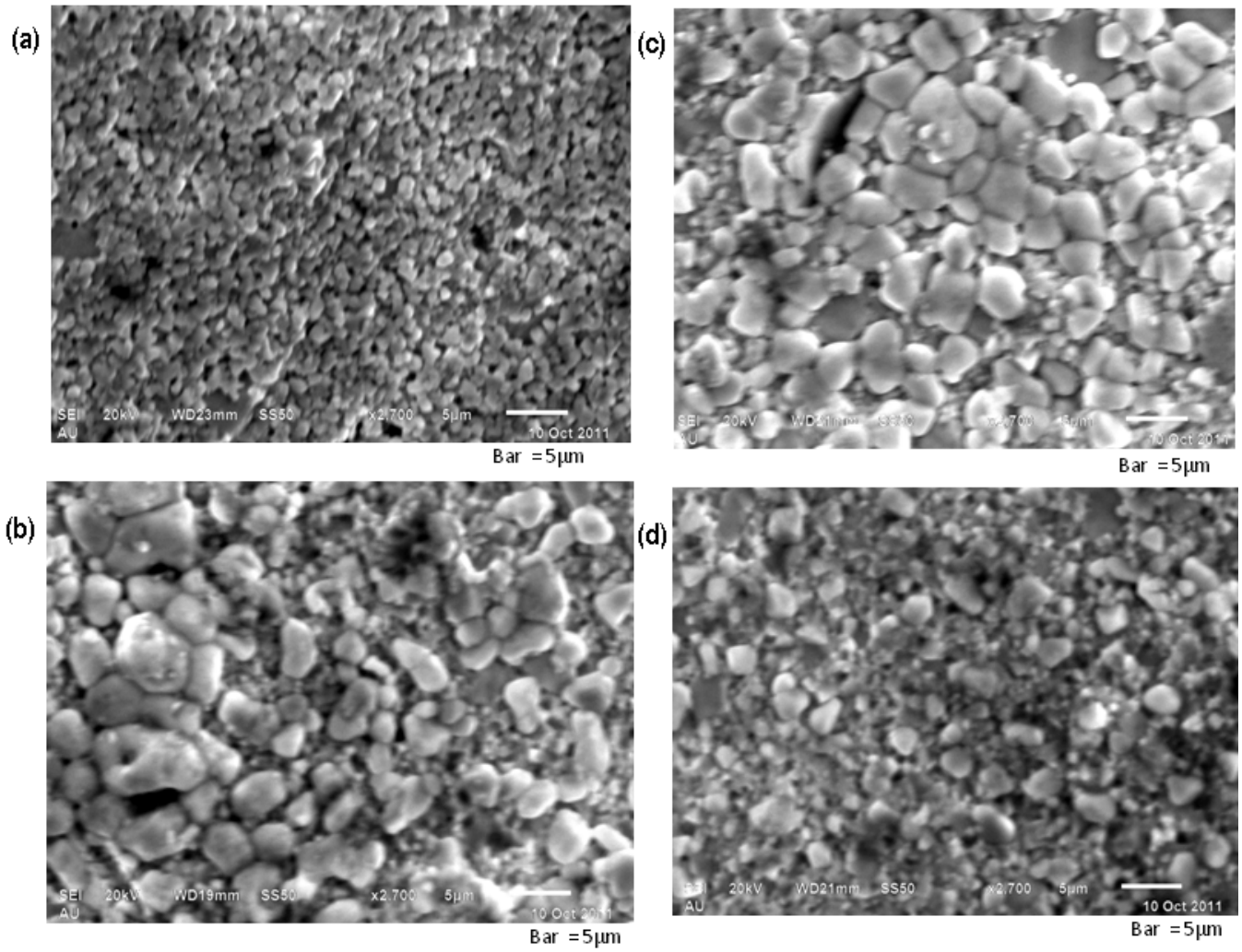

Fig. 2 SEM micrographs of $(Bi_{0.5}Na_{0.5})_{0.94}Ba_{0.06}Ti_{1-x}Sn_x)O_3$ sintered pellets at 1150^o for 2h: (a) x = 0.0 (b) x = 0.005; (c) x = 0.015 c) & x = 0.03.

4. Thermal Analysis

Fig.4 depicts the differential scanning calorimeter (DSC) measurements data taken on powder samples of BNBTSx for x = 0.0, 0.005, 0.015 and 0.03. The DSC curves showed two small endothermic peaks at different temperatures, which indicate the influence of tin doping on the two anomalous transition temperatures. The depolarization temperature (T_d) measured for the base material, bismuth sodium barium titanate, coincides with earlier report while the Curie temperature lowered by about 10^{o}C [14]. The ferroelectric to antiferroelectric (FE-AFE) and ferroelectric to paraelectric (FE-PE) transitions for all the above compositions were observed at 88ºC, 92ºC, 88ºC, 88 ºC and 275ºC, 292 ºC, 342ºC, 338ºC respectively. Here, on the temperature at which the transition between anti-ferroelectric phases to ferroelectric phase occurred there is no significant changes observed with increase in tin concentration.

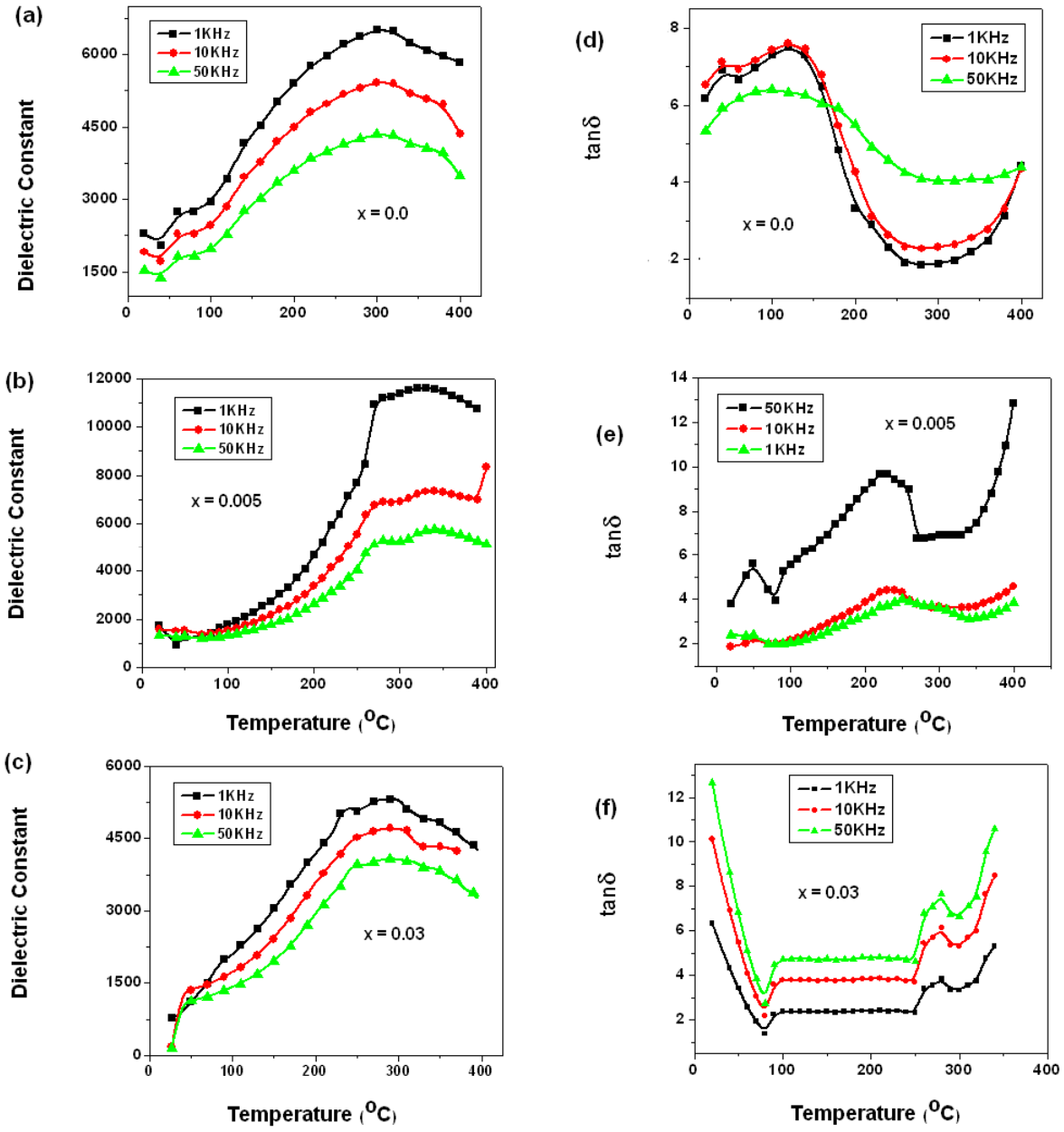

Fig. 3 Variation of dielectric constant and loss tangent versus temperature for $(Bi_{0.5}Na_{0.5})_{0.94}Ba_{0.06}Ti_{1-x}Sn_xO_3$ samples corresponding to x = 0.0, 0.005 and 0.03 measured at 1, 10 and 50 KHz frequencies.

But, in the case of ferroelectric to paraelectric transition the increase in tin concentration from x = 0.0 0.to 0.03 would change the Curie temperature by about 63°C.

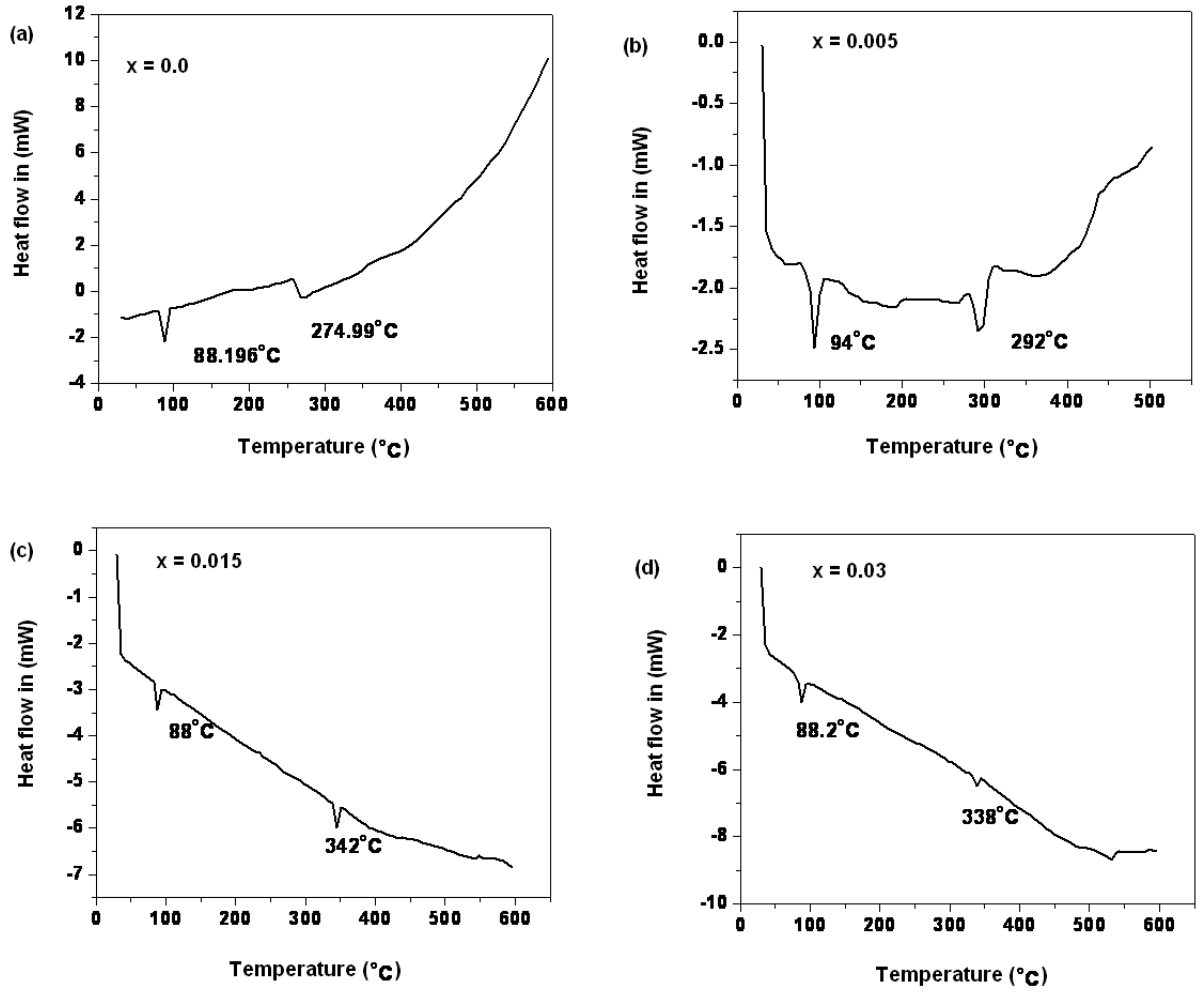

Fig.4 DSC measurements of $(Bi_{0.5}Na_{0.5})_{0.94}Ba_{0.06}Ti_{1-x}Sn_x)O_3$ ceramic powder samples with x = 0.0, 0.005, 0.015 and 0.03 in the temperature range of 27°C to 600°C up on heating.

5. Impedance Studies

Fig. 5(a-c) shows variation of the real part of the impedance (Z') with frequency and concentration at temperatures above 350°C. The magnitudes of the real and imaginary part of the impedance are decreasing as a function of the applied frequency and there is no Z"max (peak) observed at the temperature below 350°C in BNBTSx systems in the studied range. It is observed that the magnitude of Z' decreases with the increase in frequency and temperature,

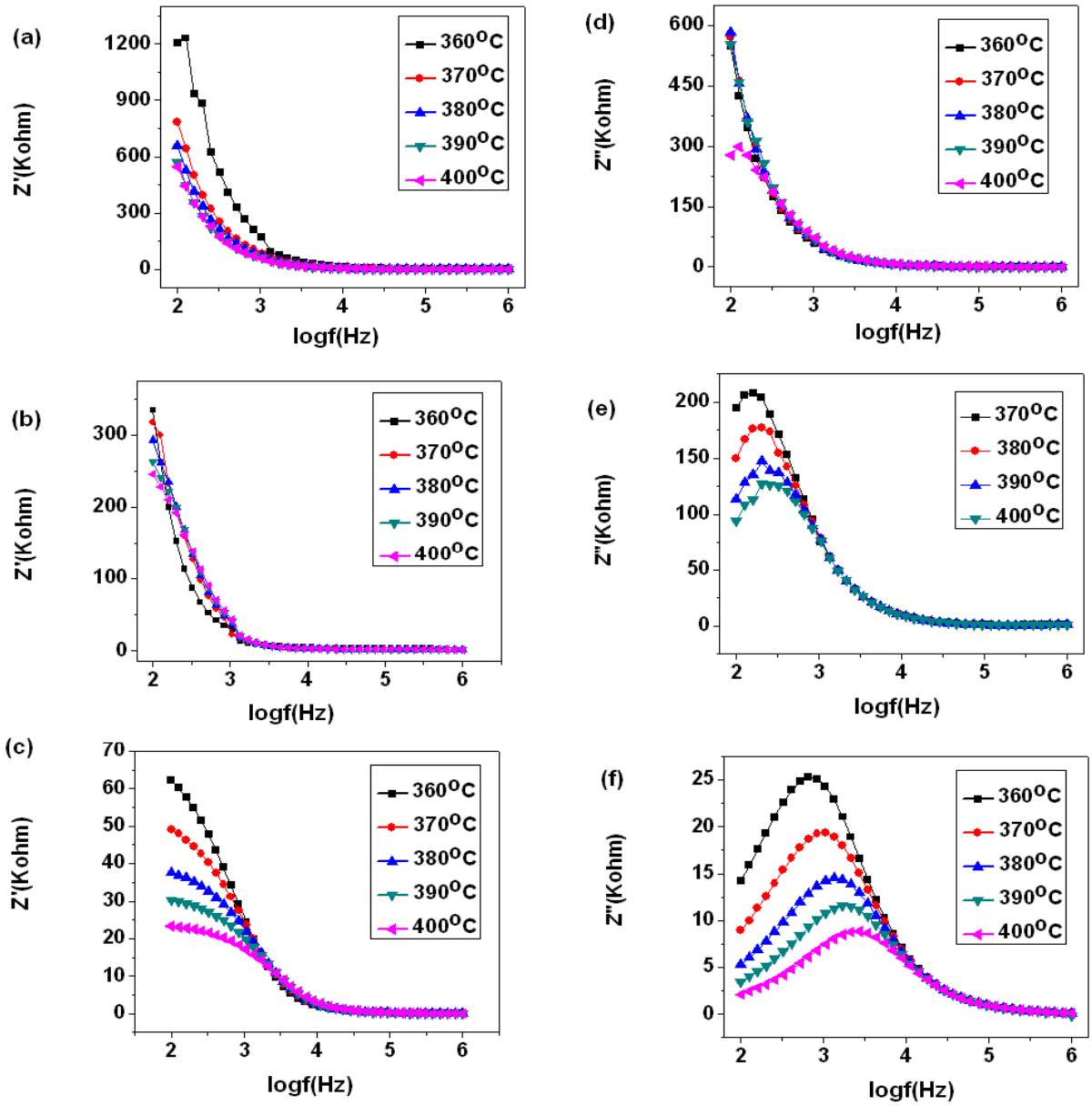

Fig.5 (a-f) shows the dependence of the real and imaginary part of impedance against frequency for BNBTSx samples with x = 0.0, 0.005 and 0.03 at various temperatures**.**

Indicating a decrease in resistivity of BNBTSx ceramic samples with frequency where x =0.0, 0.005 and 0.03. The Z' curves merged at high frequency for all temperatures. Fig.5 (d-f) shows the variation of imaginary part of impedance Z" with frequency at different temperatures. The curves show that the Z" value reaches a maxima (Z" max) above 350^{o}C and the peak shifts to higher frequency side with increasing temperature and concentration of tin. The calculated activation energy values of tin modified BNBT from its Arrhenius plots of peak frequency ($\log\omega_{max}$) as a function of 1000/T(K^{-1}) is found to be 0.85, 1.05 , 0.42eV for 0.5%, 1.5% and 3% tin substituted samples respectively.

Fig.6 show the frequency dependence of Z' and Z" (Nyquist plot) of BNBTSx samples for x = 0.0, 0.005 and 0.03 at the temperature of 400^{o}C in the frequency range 100Hz -1MHz and Argand diagram (imaginary part of the complex impedance (Z*) versus its real part) to study the influence of tin concentration on bulk resistance and relaxation frequency. These plots indicate the existence of impedance relaxation phenomena (a continuous decrease of real part of impedance (Z') associated with a maximum of imaginary part of impedance (Z") at the relaxation

frequency). It clearly shows the shift of peak frequency toward the right with increase in tin concentration along with and gradual decrease of Z' and Z" values. The inset Argand diagram of BNBTSx at the temperature of 400^{o}C also indicates as the radius of the arc (or bulk resistance) of BNBTSx samples decreased with concentration of tin diffused in to the lattice of BNBT structure. The impedance plot shows depressed semicircular arcs with their centers lying below the real axis rather than on the real axis.

6. Conductivity Studies

Frequency dependence of ac conductivity above 350^{o}C for BNBTSx (x = 0.005, 0.015 and 0.03) ceramic samples are shown in figure 7. At temperatures <350^{o}C, the frequency independent plateau is not clearly observed in the studied frequency range due to high resistance of the material, while at high temperature this plateau is coming out. The frequency independent plateau at a low frequency for higher temperatures is attributed to the long-range translational motion of ions contributing to dc conductivity (σdc). The observed frequency independent dc conductivity at higher temperature was explained by Funke [15] in the jump relaxation model (JRM). Due to, the increased (n>1) of conductivity spectra at high frequency ac conductivity could not be modeled using simple Jouscher's power law but could be modeled using double power law for tin substituted BNBT [16-18];

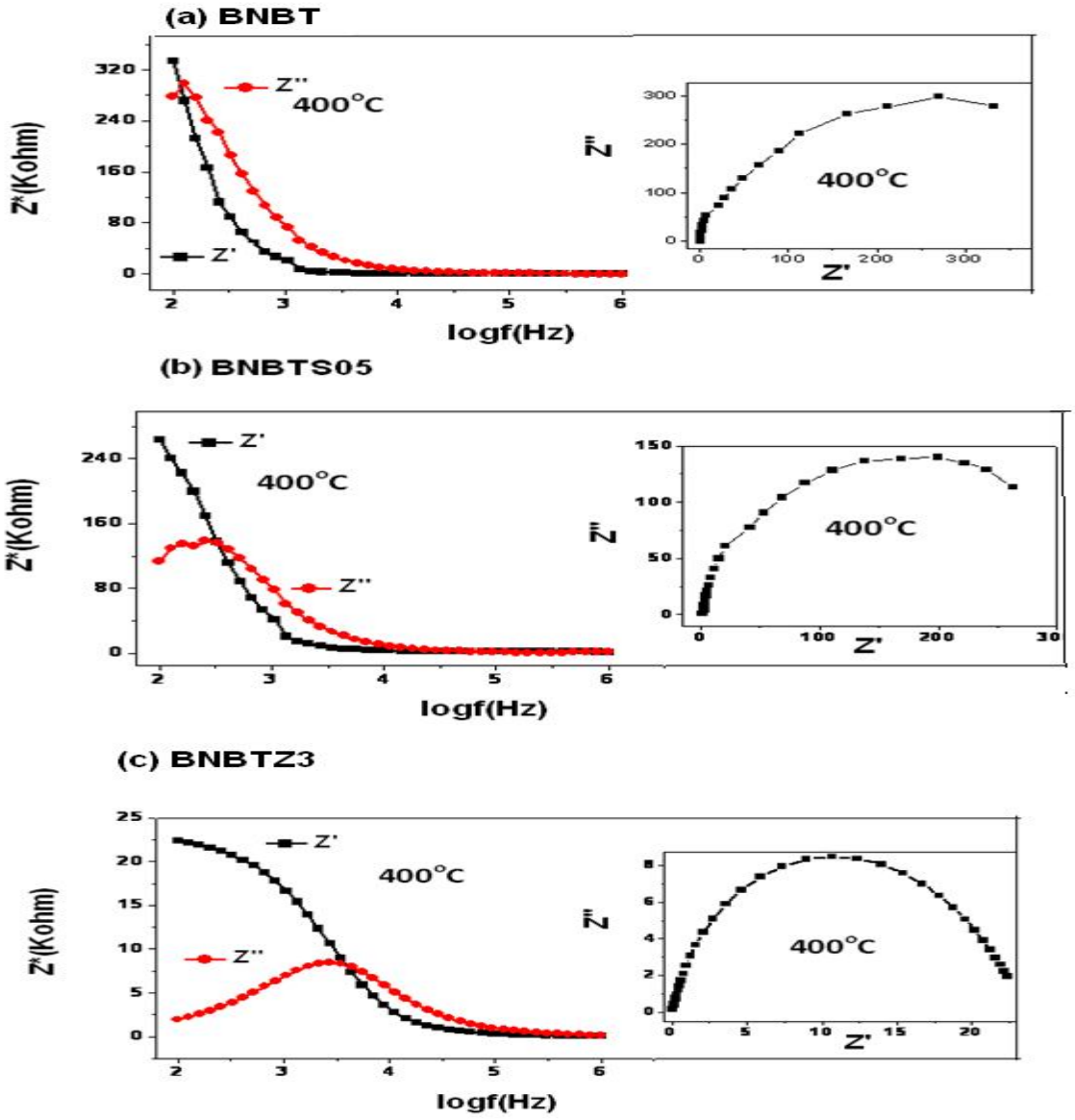

Fig. 6 Frequency dependence of Z' and Z" ; (Inset) Corresponding Argand diagram of (a)BNBTS0 , (b) BNBTS05, (c) BNBTS3 ceramic samples at temperature of 400^{o}C.

$$\sigma(\omega) = \sigma_0 + A_1\omega^{n_1} + A_2\omega^{n_2}$$

The term (σ_0) corresponding to the translation hopping gives the long-range electrical transport (i.e., dc conductivity) in the long time limit. The second one $A_1\omega^{n_1}$ was assigned to the translational hopping motion (short-range hopping). Whereas the one at high frequencies $A_2\omega^{n_2}$ is associated to a localized or reorientational hopping motion [15]. The inset of Fig.8 c showed the temperature dependences trend and values of n_1 and n_2 for BNBTZ3 sample in the studied range of temperature. Furthermore, the value of n_1 approaches zero at higher temperatures, indicating that dc conductivity dominates at higher temperatures in the low frequency region and obeys Josher's power law [19]. The observed values of n_1 within 0–1 and the values of n_2 in between 1 and 2 for BNBTS05, BNBTS1.5 and BNBTS3 ceramics satisfy the double power law.

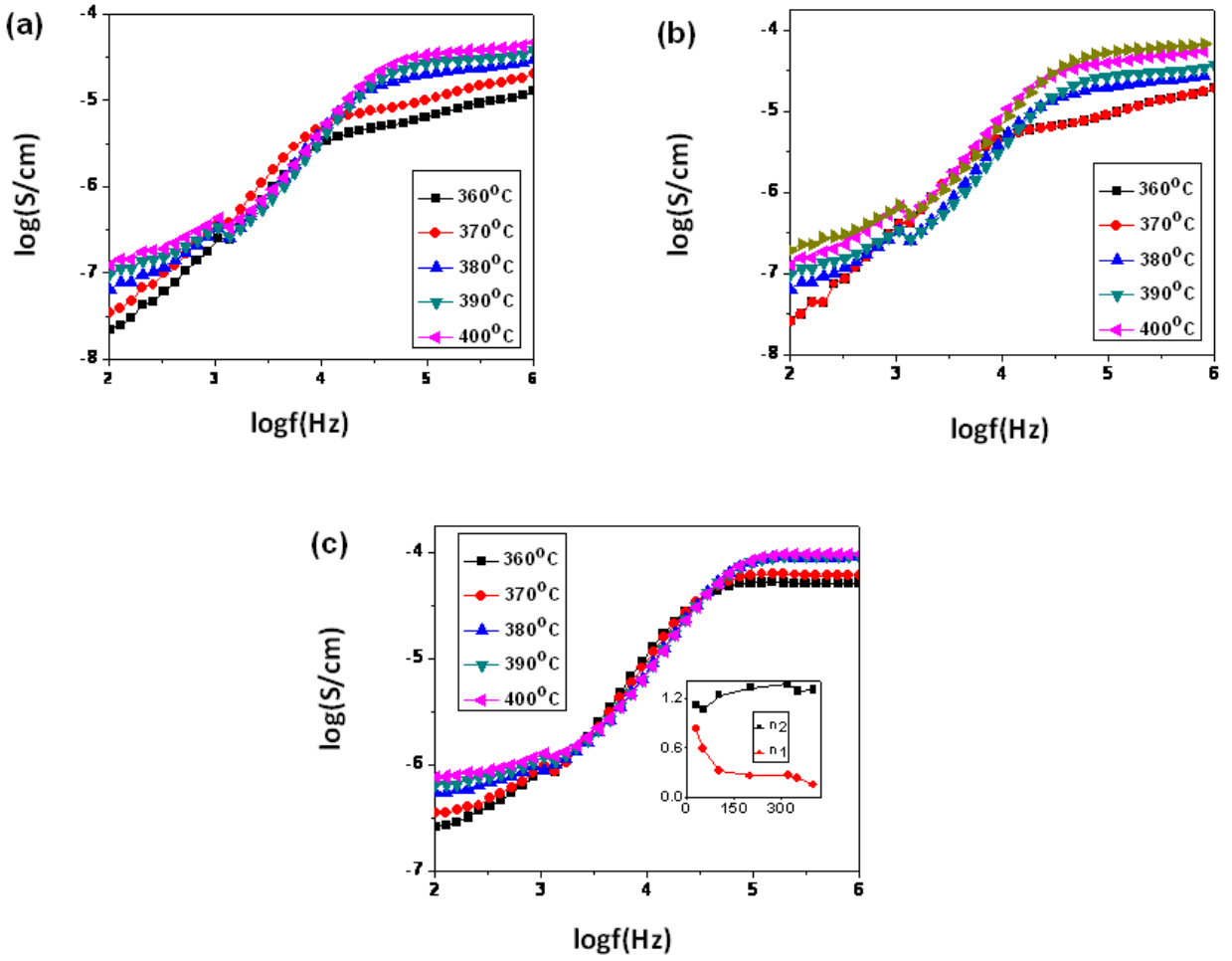

Fig.7 Dependence of ac conductivity on frequency at various temperatures of BNBTSx: (a) x = 0.005, (b) x = 0.015, (c) x = 0.03 .The inset in Fig.7c showed temperature dependence index (n) for BNBTZ3.

Fig. 8 shows the variation of conductivity as a function of temperature measured at different frequencies for pure and Sn doped BNBT samples. The a.c and d.c conduction activation energies have been calculated for three different temperature regions at different frequencies using Arrhenius relation and the values are given in the table 1. The data in the table show that the dc activation energies are greater than that of ac at most point. This is because the dc conductivity is caused by the transportation of conducting species over a long distance rather than reorientational mechanism as in ac conductivity via dipole formation.

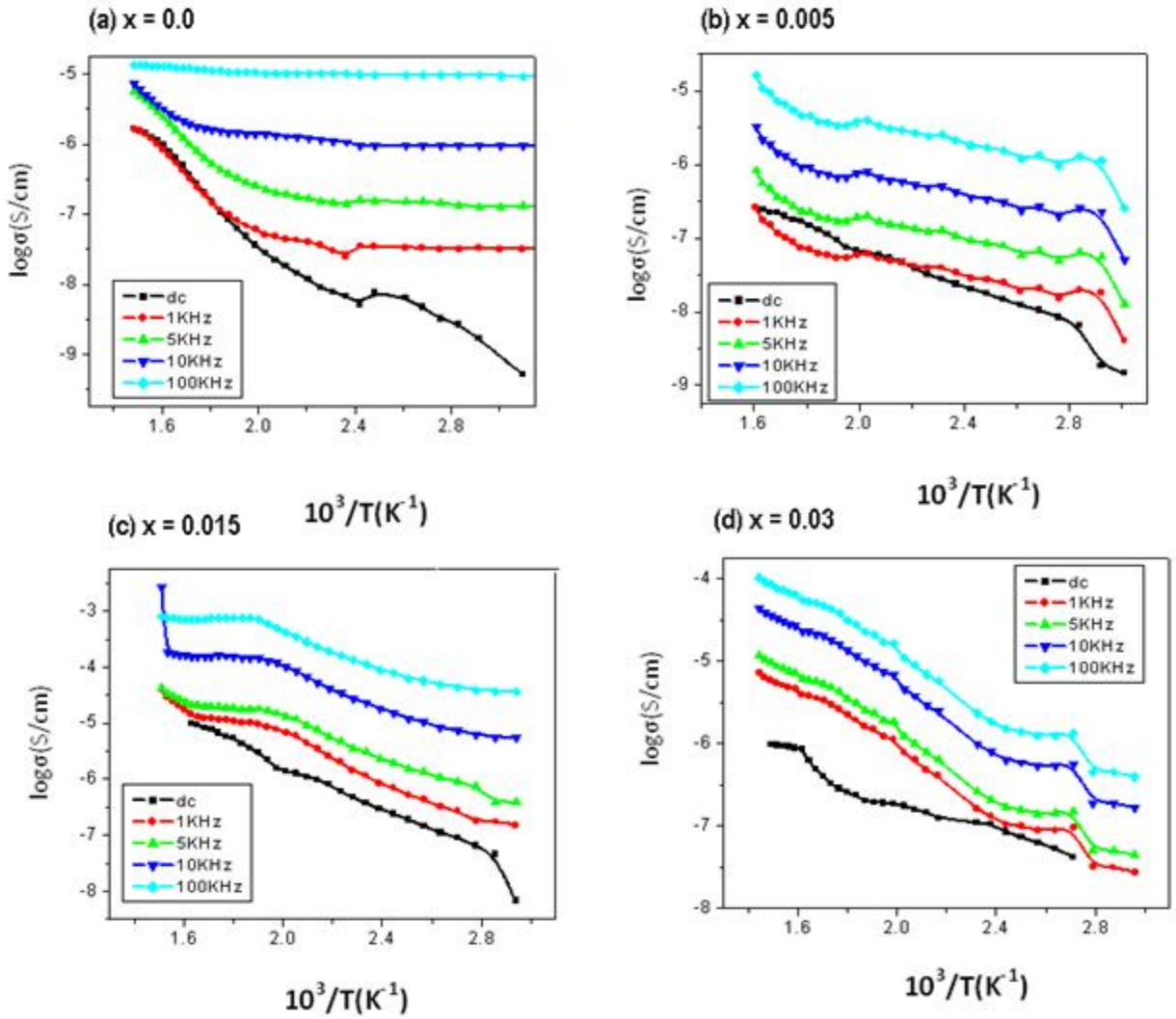

Fig.8(a-d) Conductivity vs 10^3T^{-1} of $(Bi_{0.5}Na_{0.5})_{0.94}Ba_{0.06}Ti_{1-x}Sn_x)O_3$ for x = 0.0, 0.005, 0.015 and 0.03 at the frequencies of 1, 10, 50, 100KHz.

Table.1 Activation energies in the units of electron volts of pure and Sn doped BNBT ceramic samples for three different temperature regions.

Composition	Frequency	Temperature(°C)		
		30-150°C	150-300°C	300-400°C
BNBTS0	dc	0.125	0.195	0.85
	1KHz	0.232	0.115	0.205
	10KHz	0.221	0.109	0.141
BNBTS05	dc	0.04	0.41	0.89
	1KHz	0.23	0.53	0.69
	10KHz	0.11	0.21	0.49
BNBTS1.5	dc	0.12	0.67	1.13
	1KHz	0.11	0.34	0.39
	10KHz	0.07	0. 27	0.44
BNBTS3	dc	0.08	0. 71	0.82
	1KHz	0.10	0.28	0.42
	10KHz	0.10	0.11	0.31

7. Conclusion

Samples with compositions $(Bi_{0.5}Na_{0.5})_{0.94}$ $Ba_{0.06}$ $(Ti_{1-x}Sn_x)O_3$, for x = 0.0, 0.005, 0.015 and 0.03 were synthesized by conventional solid state method. All samples showed formation of single phase rhombohderal structure. Substitution of Sn in B site led to enhanced grain growth. Sn substitution of 0.005 led to higher dielectric properties, while further increase in Sn concentration led to decrease in dielectric constant compared to pure BNBT. An overall increase in a.c. conductivity has been observed with Sn substitution. The bulk resistance (Rb) was shown to decrease with increasing temperature indicating a negative temperature coefficient of resistance (NTCR) behavior. Activation energies (Ea) have been calculated from the slope of the log σ versus 10^3/T curves.

Acknowledgement

This research was supported by Ministry of Education of Federal Democratic Republic of Ethiopia.

REFERENCES

1. Smolenskii, G.A.; Isupov, V.A.; Agranovskaya, A.I.; Kraink, N.N.; Sov. Phys. Solid State. **2**, 2651, (1961)**.**
2. Takenaka, T.; Maruyama, K.; Sakata, K. Jpn.; J. Appl. Phys. **30**, 2236,(1991).
3. Chu, B. J.; Chen, D. R.; Li, G. R.; Yin, Q. R.; J. Eur. Ceram. Soc. **22**, 2115, (2002).
4. Takenaka, T.; Sakat, K.; Ferroelectrics. **95**, 153, (1989).
5. Li, Y. M.; Chen, W.; Zhou, J.; Xu, Q.; Sun, H.; Xu, R. X. ;Mater. Sci.Eng. B. **112[5]**, 115, (2004).
6. Nagata, H.; Koizumi, N.; Kuroda, N.; Igarashi, I.; Takenaka, T.; Ferroelectrics. **229[1-4]**, 273, (1999).
7. Wu, Y. G. ; Zhang, H. L.; Zhang, Y.; Ma, J. Y.; Xie, D. H.; J. Mater. Sci. **38[5],** 987, (2003).
8. Chen, Z. W.; Shui, A.; Lu, Z. Y.; Liu, P. G.; J.Ceram. Soc. Jpn, , **114[1334]**, 857, (2006).
9. Zuo, R.; Wang, H.; Ma, B.; Li, L.; J. Mater. Sci. Mater Electron. **20**, 1140, (2009).
10. Hao, J. J.; Wang, X. H.; Gui, Z. L.;. Li, L. T.; *Rare Metal Materials and Engineering*, **32,**438, (2003).
11. Herabut, A.; Safari, A.; *J. Am. Ceram. Soc.*, **80[11]**, 2954, (1997).
12. Lin, Y.; Zhao, S.; Cai, N.; Wu, J.; Zhou, X.; Nan. C.; *Mater. Sci. Eng. B* **99**, 449, (2003).
13. Suryanarayana, C.; Grant, M. N. X-Ray Diffraction a Practical Approach, Plenum Press, New York, **1998**, 207-221.
14. Xu, C.; Lin, D.; Kwok, K. W.; Solid- State Sci., **10[7]**, 934, (2008).
15. Funke, K.; Prog. Solid. State Chem. **22**,111, (1993).
16. Almond, A.P.; West, A.R.; Grant, R.J.; Solid State Commun. **44**, 27, (1982).
17. Barramco A.P.; Gutierrez-Amador, M.P.; Valenzuela, R. Appl. Phys. Lett.,**73**, 2039,(1998).
18. Ortega, N.; Kumar, A.; Bhattacharya, P.; Katiyar, R.S.; Phys. Rev., B **77,** 014111,(2008).
19. Jonscher A.K.; Nature. **267**, 673, *(*1977).